Non-peer-reviewed preprint submitted to EarthArXiv. Version 1.2, October 2026. The manuscript has also been submitted to *Remote Sensing Letters* for peer review. Version 1.1: https://doi.org/10.31223/X5SC0B. Version 1 (8 October 2026), with its data and code: https://doi.org/10.5281/zenodo.23241823.

Same computation, different scenes: a single-site comparison of Sentinel-2 L2A composites from Google Earth Engine and Microsoft Planetary Computer

Heiber Alexander Pantevez Villamil[1,2]

[1] Doctoral Program in Agroecology, Facultad de Ciencias Agropecuarias, Universidad Nacional de Colombia, Sede Palmira, Palmira, Colombia

[2] Facultad de Ciencias Agrarias, Universidad Nacional de Colombia, Sede Bogotá, Bogotá, Colombia (internal mobility)
ORCID: https://orcid.org/0000-0003-1797-0057
Correspondence: hapantevezv@unal.edu.co

Abstract. Google Earth Engine (GEE) and Microsoft Planetary Computer (MPC) distribute Sentinel-2 Level-2A surface reflectance, and their outputs can be combined in one time series. Over a 73 ha cattle farm in northern Colombia, we tested whether the two platforms yield the same parcel-scale vegetation and water indices and, where they differ, whether the difference originates in the product (the L2A scene), the processing chain (masking, 3 × 3 smoothing, NDVI, EVI, NDWI and monthly median) or the scene universe (which acquisitions enter a composite). For the ten pairs in which both platforms served the same product, scene classification and harmonised reflectance matched in every comparable pixel, and the same chain run locally or server-side in GEE agreed within 10^{-6}. The catalogues, however, did not hold the same scenes. Between June 2024 and April 2025, 10 of 146 scene–tile records existed only in GEE, six of them Sentinel-2C records from around the satellite's entry into operations, and none only in MPC. In 22 of 136 common records, all from June–July 2024, the catalogues held different L2A generations; of the ten such pairs with valid pixels, one had a different cloud mask. Adding the GEE-only scenes shifted mean monthly NDVI over the farm by −0.0005 (December 2024) and −0.0087 (January 2025), and by up to −0.028 in a public 1 km² demonstration area (January 2025). For the operations tested, the platforms are computationally equivalent, but combining them requires reconciling scene inventories. The reconciliation table, composite scene lists and open-source tools are released.

Keywords: Sentinel-2; Google Earth Engine; Microsoft Planetary Computer; interoperability; reproducibility; STAC; scene inventory; provenance

1. Introduction

Cloud platforms have changed how Earth observation data are accessed and processed. Google Earth Engine (GEE) couples a public data catalogue with server-side computation (Gorelick et al., 2017), while Microsoft Planetary Computer (MPC) exposes its catalogue through the SpatioTemporal Asset Catalog (STAC) standard (Open Geospatial Consortium, 2025) and cloud-optimised files that users process with their own tools (Microsoft, n.d.). Reviews of these platforms compare architecture, data access and computing models (Gomes et al., 2020), and reviews of GEE document a large and growing body of applications (Amani et al., 2020; Tamiminia et al., 2020). Initiatives such as openEO aim to make the same process give the same result on different back-ends (Schramm et al., 2021). Less attention has been given to whether the same product, retrieved from two platforms, leads to the same numbers, and whether the platforms hold the same products at all.

The question is practical. Long parcel-scale time series need hundreds of scenes, and quota, memory or processing limits can make it convenient to split production across platforms. If one year is computed in GEE and the next from MPC, a change in an index at the boundary may reflect a real change in land cover or merely the change of source. Changes of data source are known to affect index continuity (Roy et al., 2016) and can be mistaken for real change by break-detection methods (Verbesselt et al., 2010; Zhu & Woodcock, 2014). For Sentinel-2 L2A (Drusch et al., 2012), three factors can make the platforms differ even when they distribute the same mission data. First, since processing baseline 04.00, in operation from 25 January 2022, reflectance values carry an additive offset stored in each product's metadata (European Space Agency, n.d.); GEE removes it in its harmonised collection (Google, n.d.), whereas MPC distributes the original values and leaves the offset to the user (Bunting, 2022). Second, ESA reprocesses acquisitions, so a given acquisition may exist in several L2A generations (Enache et al., 2023). Third, each platform ingests new and reprocessed products through its own pipeline; we found no published ingestion schedule for either.

This note asks whether GEE and MPC give the same parcel-scale Sentinel-2 L2A indices when the processing chain is held constant and, when results differ, whether the difference comes from the product, the implementation or the set of scenes each catalogue holds. In the terms of Kedron et al. (2021), it is a reproducibility test across computational environments. We answer it for one farm with a design that isolates each layer, report how often catalogue differences occurred over eleven months, quantify their effect on two monthly composites and release the data and tools used.

2. Data and methods

2.1 Study site and grid

The site is a 73 ha cattle farm in the department of Cesar, northern Colombia, located in the overlap of Sentinel-2 MGRS tiles T18PXS and T18PYS, so that each acquisition can appear twice, once per tile. The farm geometry is not published, to protect the landowner's privacy; a public demonstration area in the same tile overlap is released with the data (Section 2.3). All analyses used a fixed grid in EPSG:9377 (MAGNA-SIRGAS

2018 / Origen-Nacional; IOGP, n.d.) at 10 m, with pixel-centre membership, giving 7,348 pixels inside the farm.

2.2 Products and processing chain

We used the GEE collection `COPERNICUS/S2_SR_HARMONIZED` and the MPC collection `sentinel-2-l2a`, retrieving bands B02, B03, B04, B08 and the scene classification layer (SCL) produced by Sen2Cor (Main-Knorn et al., 2017). Reflectance was computed as max(DN + BOA_ADD_OFFSET, 0) / BOA_QUANTIFICATION_VALUE, with the offset read per band from each MPC product's metadata (−1,000 in all bands of our scenes) and already applied in the GEE collection. SCL classes 2, 4, 5, 6 and 7 were considered valid, with SCL brought from 20 m to 10 m by nearest neighbour. Classes 2 (dark area) and 7 (unclassified) were kept to avoid discarding dark or unclassified clear pasture, at the cost of admitting some shadow and cloud-edge errors (Baetens et al., 2019); the rule was identical for both platforms. A pixel was valid when its SCL class was valid and all four bands held native data. Reflectance was averaged over valid pixels in a 3 × 3 window, including valid neighbours outside the farm, before computing NDVI (Rouse et al., 1974), EVI (Huete et al., 2002) and NDWI (McFeeters, 1996). Monthly composites were per-pixel medians of each index. Each scene–tile record entered the median as one observation, so an acquisition present in both tiles contributed twice; composite values therefore depend on which and how many observations are available (White et al., 2014).

2.3 Design

We distinguished three layers at which the platforms could diverge (Table 1) and tested each one separately. The investigation was diagnostic rather than a sample: the scene pairs and months below were chosen after an initial discrepancy between a monthly composite exported from GEE and the same composite computed locally for January 2025.

Table 1. Layers of comparison and how each was tested.

Layer	Definition	Test
Product	The L2A scene, identified by product identifier, datatake and processing baseline	Identity metadata; pixel-wise comparison of SCL and harmonised reflectance on the native grid
Processing chain	Masking, 3 × 3 smoothing, indices and monthly median	Same scenes processed locally from each platform's raw files and server-side in GEE with identical operations
Scene universe	Which acquisitions enter a composite	Reconciliation of both catalogue inventories by acquisition and tile over eleven months, and effect on monthly composites

Product equivalence. Eleven scene pairs from June 2024, December 2024 and January 2025 were classified as E1 when both platforms served the same product identifier, and as E2 when they served different L2A generations of the same acquisition. For each pair we downloaded raw bands and SCL from both platforms on the same native UTM window and compared them pixel by pixel.

Processing equivalence. For the ten December 2024 and January 2025 scenes we compared per-scene indices and monthly medians computed (i) locally from GEE raw files, (ii) locally from MPC raw files and (iii) server-side in GEE with the same operations, downloaded on the same 10 m grid. Agreement was assessed as the fraction of pixels with absolute difference ≤ 10^{-6}. Local–local comparisons were made in float64 and comparisons involving GEE downloads in float32.

Catalogue reconciliation. For June 2024 to April 2025, we listed every GEE image and MPC item whose footprint intersected the farm and matched them by acquisition key: the datatake identifier without its processing-baseline suffix, plus the MGRS tile. Each record was labelled as present in both catalogues, only in GEE or only in MPC, and common records were labelled E1 or E2 by product identifier. For E2 records, SCL from both generations was compared on the native 20 m grid without resampling. Catalogues were queried on 24 September 2026. For every record the released table lists both identifiers, the sensing and generation times, the processing baseline and the cloud cover reported by each catalogue.

Effect on composites. For December 2024 and January 2025, monthly medians were computed with the same local engine for two scene universes: the scenes common to both catalogues and the full GEE inventory. Records with scene cloud cover above 20% were excluded; the filter was applied per scene–tile record, using GEE's `CLOUDY_PIXEL_PERCENTAGE` and MPC's `eo:cloud_cover` only for records absent from GEE (there were none), and these properties describe the whole tile rather than the farm. We report the bias (mean of GEE minus common) and the mean absolute error (MAE) over the farm, with a 95% confidence interval for the bias from a block bootstrap (10 × 10 pixel blocks, 2,000 resamples) that accounts for spatial autocorrelation, the 5th and 95th percentiles of the per-pixel difference and the fraction of pixels whose absolute difference exceeds 0.01 and 0.02.

Demonstration area. To provide a reproducible case that does not reveal the farm, the reconciliation, the E2 analysis and the composite comparison were repeated over a public 1 km × 1 km square (9,970 pixels) in the same T18PXS/T18PYS overlap, located away from the farm. Here the composite comparison covered every month with GEE-only records (September and December 2024, January and February 2025).

2.4 Workflow, parameters and software

Figure 1 summarises the study design (panel A) and the data flow of the released toolkit (panel B), with the inputs and outputs of each phase, the decision gates and the feedback from verification to catalogue reconciliation. Table 2 lists every parameter needed to replicate the analysis. Phase 0 (inputs and grid) is shared by the three scripts; phases 1–2 are implemented in `reconcile_catalogues.py`, phase 3 in `e2_frequency.py`, and phases 4–9 in `composite_impact.py`. The toolkit also computes annual composites as a multivariate medoid of monthly index triplets, adapted from Flood (2013); annual composites were not evaluated in this study.

Table 2. Parameters required to replicate the analysis.

Item	Value
Collections	GEE `COPERNICUS/S2_SR_HARMONIZED`; MPC `sentinel-2-l2a` (STAC API v1)
Period and query date	1 June 2024 – 30 April 2025 (reconciliation); catalogues queried 24 September 2026
Bands	B02, B03, B04, B08 (10 m); SCL (20 m)
Radiometry	ρ = max(DN + BOA_ADD_OFFSET, 0) / BOA_QUANTIFICATION_VALUE (10,000); offset read per band (−1,000 in our scenes), already applied in GEE
Valid SCL classes	2 (dark area or topographic shadow), 4 (vegetation), 5 (not vegetated), 6 (water), 7 (unclassified)
Grid	EPSG:9377, 10 m, origin at multiples of 10 m; nearest-neighbour warping; pixel-centre membership (7,348 pixels)
Validity	Valid SCL and native data in all four bands; nodata −9999 or separate mask band
Neighbourhood	3 × 3 mean of valid pixels before indices, neighbours outside the farm included; centre must be valid
Indices	NDVI; EVI (G = 2.5, C1 = 6, C2 = 7.5, L = 1); NDWI (McFeeters)
Monthly reducer	Per-pixel median per index (mean of the two central values when n is even); one observation per scene–tile record
Scene filter	Scene cloud cover ≤ 20% per scene–tile record (GEE `CLOUDY_PIXEL_PERCENTAGE`, else MPC `eo:cloud_cover`)
Reconciliation key	Datatake identifier without `_Nxx.xx` suffix + MGRS tile; E1/E2 by product identifier
Equivalence tolerance	Absolute difference ≤ 10^{-6}

Software and environment. All computations ran in Python 3.12.3 inside a Linux Docker container, from JupyterLab and the terminal, with earthengine-api 1.7.10, pystac-client 0.9.0, planetary-computer 1.0.0, rasterio 1.5.0 (GDAL), geopandas 1.1.2, shapely 2.1.2, NumPy 2.3.5 and pandas 2.3.3, following common practice for reproducible geoscience computing (Nüst & Pebesma, 2021). Every output records its parameters and inputs: reconciliation tables keep the query date, and each composite stores a per-pixel observation count and the SHA-256 hash of its scene list. The data release includes these tables, the scene lists of each composite and a public demonstration area of interest on which the tools can be run end to end.

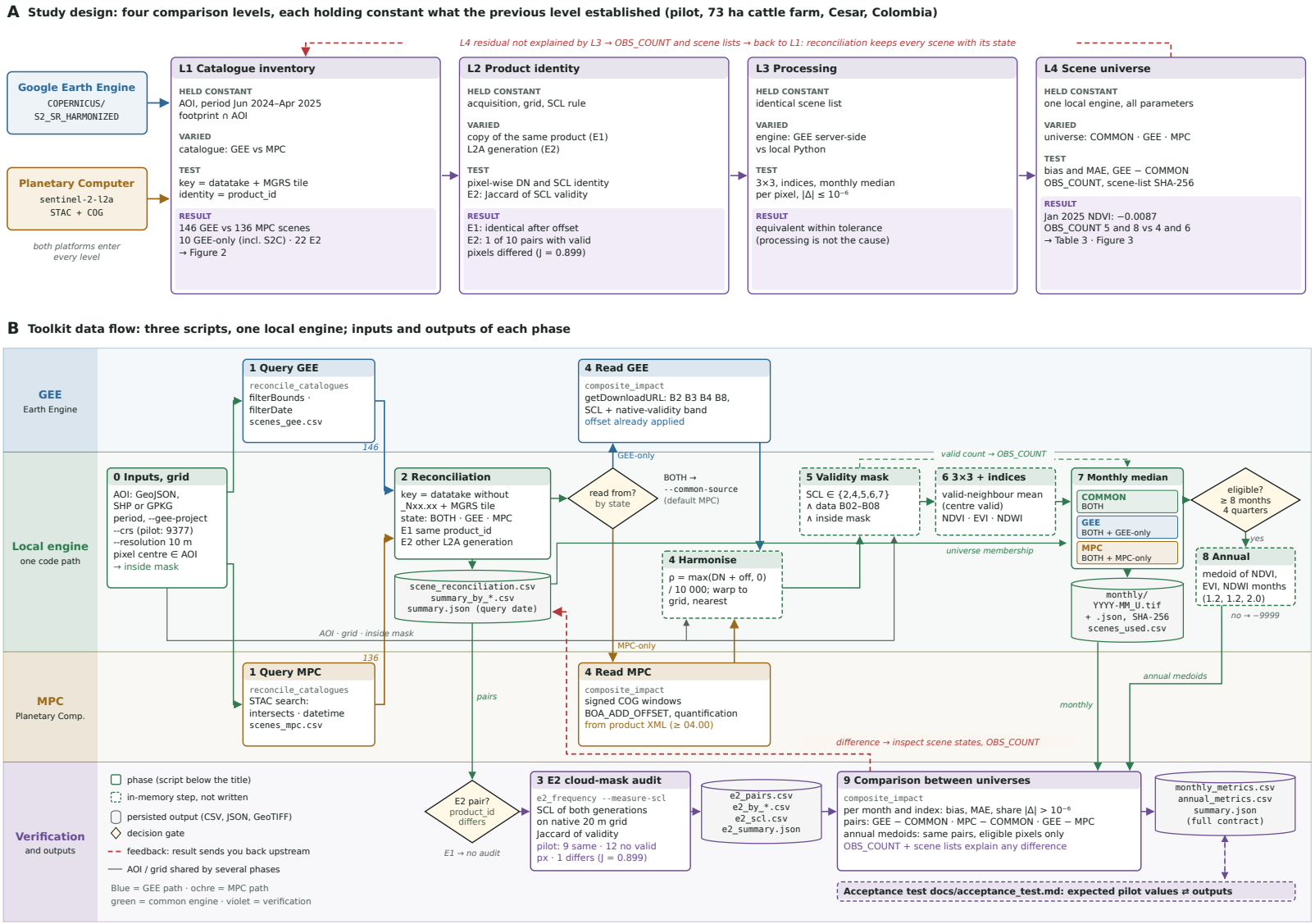


Figure 1. (A) Study design: four comparison levels, each isolating one source of difference while holding constant what the previous level established. Levels 1 and 4 correspond to the scene-universe layer of Table 1, and levels 2 and 3 to the product and processing layers. The dashed red arrow marks the feedback that redirected the investigation from processing to the scene catalogues. (B) Data flow of the released toolkit in swimlanes (GEE, local engine, MPC, verification). Phases are numbered 0–9; each shows its operation, inputs and outputs, with the script below its title. Cylinders are files written to disk, dashed boxes are in-memory steps and diamonds are decision gates. The reconciliation state of each scene decides which catalogue it is read from and which scene universes it enters. Values from this study appear in italics or after "pilot". Python libraries and versions are given in Section 2.4.

3. Results

3.1 Identical products give identical data

Ten of the eleven pairs were E1. In all ten, SCL arrays were identical and the relation $DN_{GEE} = \max(DN_{MPC} - 1000, 0)$ held in every comparable pixel, confirming that both platforms serve the same content and differ only in the documented offset convention. Comparable pixels exclude 31 pixels in two scenes affected by the nodata artefact described below. Indices computed locally from either source differed by at most 4.4×10^{-16}. The remaining pair (1 June 2024, T18PXS) was E2: of the 2,854 pixels valid in either generation within the native UTM window used for this pair, which extends beyond the farm, the two disagreed on 288 (103 valid only in MPC, 185 only in GEE; Jaccard index 0.899). All disagreements came from SCL, 79% of them next to SCL class boundaries, and none from the native masks of the spectral bands. This pattern is consistent with Sen2Cor mask errors concentrating at cloud and shadow edges (Baetens et al., 2019).

The apparent mask disagreement in those 31 pixels was not a product difference. In our downloads, harmonisation in GEE produced zero values in the blue band where MPC digital numbers were below 1,000 (the catalogue page documents the shift of 1,000 but not this clipping); storing the GEE download as GeoTIFF with nodata = 0 turned those zeros into missing data.

3.2 The monthly processing chain is equivalent

Executed server-side in GEE, the chain reproduced the local computation in 100% of pixels for all ten scenes and three indices (maximum absolute difference 3×10^{-8}, consistent with float32 rounding). GEE's `median()` and 50th-percentile reducers matched the NumPy median in 100% of pixels, averaging the two central values when the number of scenes was even. A monthly composite previously exported from GEE did, however, differ from the local result (January 2025 NDVI bias −0.0087). Its per-pixel observation count showed 5 observations in December 2024 and 8 in January 2025, against 4 and 6 scenes in the paired set. Recomputing the GEE median with every catalogue scene over the farm reproduced the exported file in 100% of pixels. The discrepancy was therefore caused by the scenes entering the composite, not by the platform or the implementation. These tests cover per-scene indices and monthly medians; the annual medoid and the historical production workflow behind earlier GEE exports were not tested.

3.3 The catalogues hold different scene inventories

Over June 2024 to April 2025, GEE returned 146 images and MPC 136 items over the farm. All 136 MPC records had a counterpart in GEE; 10 GEE records (6.8%) had none in MPC, and no record existed only in MPC. The GEE-only records came from five acquisitions, each seen in both tiles, and all covered the whole farm, so differences in footprint geometry cannot explain their absence from MPC: 14 September 2024 (Sentinel-2A), 19 September 2024 (Sentinel-2B), and 13 December 2024, 22 January 2025 and 11 February 2025 (Sentinel-2C) (Figure 2a). MPC returned no item for any of these acquisitions when queried in September 2026. The two 13 December 2024 records

carry processing baseline 99.05 (product identifiers with `N9905`), the baseline of the preliminary Sentinel-2C dataset; the other eight GEE-only records carry baseline 05.11, the same as the common records of those months. As a result, MPC held no Sentinel-2C record over the farm before February 2025, while GEE held two in December 2024 and two in January 2025.

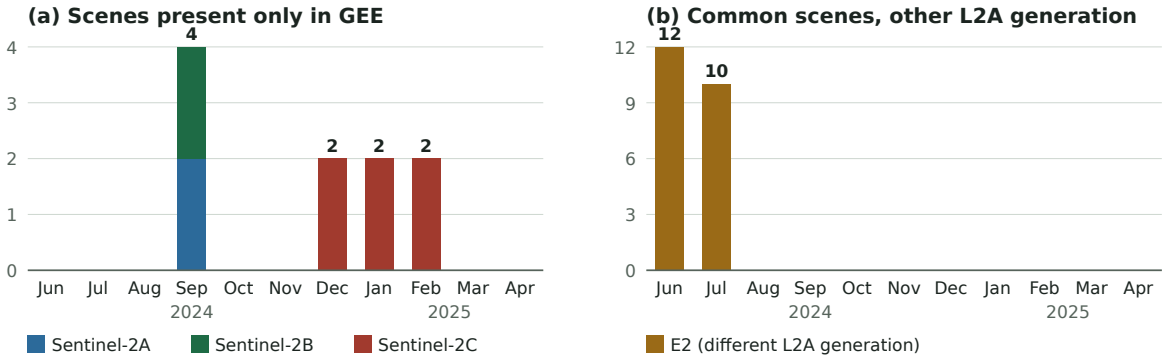


Figure 2. Catalogue reconciliation over the study farm, June 2024 to April 2025 (queries of 24 September 2026). (a) Scene–tile records present only in GEE, by month and satellite; no record was present only in MPC. (b) Records present in both catalogues but with different L2A generations of the same acquisition (E2), by month.

Among the 136 common records, 22 were E2: 12 acquired in June and 10 in July 2024, between 1 June and 21 July, all sharing the processing baseline but with different generation times (Figure 2b). This is a single episode rather than a steady rate: no E2 record occurred from August 2024 to April 2025. Over the farm, 12 of the 22 pairs had no valid pixels in either version. Of the ten pairs with valid pixels, nine had identical SCL and one differed: the June 2024 pair identified in Section 3.1 (class agreement 0.961 and validity Jaccard 0.899 on the native 20 m grid).

3.4 Effect on monthly composites

With the same engine, adding the GEE-only scenes changed the monthly medians (Table 3, Figure 3). The effect was small in December 2024, when one extra record joined four common ones: of the two tile records of the 13 December Sentinel-2C acquisition, T18PXS (scene cloud cover 4.3%) passed the per-record cloud filter and T18PYS (33.9%) did not. Its NDVI bias was indistinguishable from zero (95% CI −0.0018 to +0.0009), although 16% of pixels changed by more than 0.01. It was larger in January 2025, when the 22 January acquisition entered twice, once per tile (cloud cover 2.0% and 16.6%), accounting for 2 of the 8 inputs. The NDVI bias was −0.0087 (95% CI −0.0111 to −0.0063); 42% of pixels changed by more than 0.01 and 22% by more than 0.02, and the 5th percentile of the difference was −0.038. GEE-only records also occurred over the farm in September 2024 and February 2025, and E2 records in June and July 2024; their effect on the farm's composites was not computed, so the values in Table 3 describe the two months tested and are not bounds for the period. Scene lists, observation counts and the full per-pixel difference distributions for every index are included in the data release.

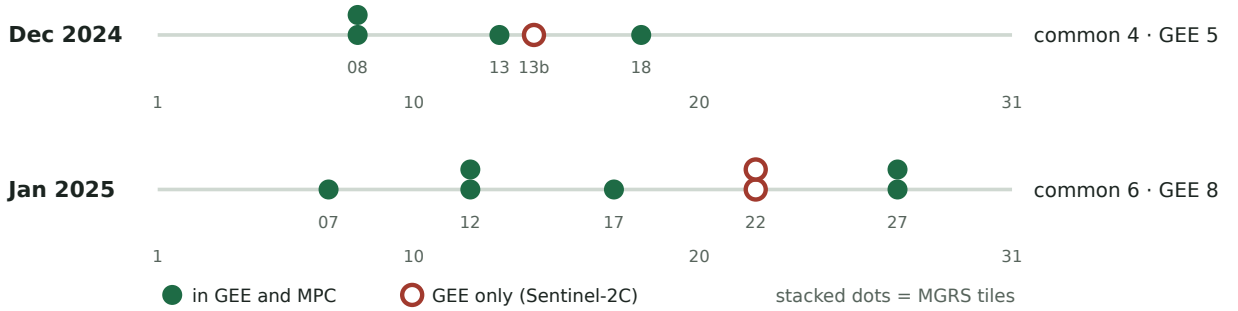


Figure 3. Scenes entering the December 2024 and January 2025 monthly composites (scene cloud cover ≤ 20%). Filled dots are scene–tile records present in both catalogues; open dots are Sentinel-2C records present only in GEE; stacked dots are the two tiles of one acquisition. On 13 December two datatakes occurred, one present in both catalogues and one Sentinel-2C datatake present only in GEE; the second is drawn offset.

Table 3. Difference between monthly medians computed with the full GEE inventory and with scenes common to both catalogues (same engine, 7,348 farm pixels).

Month	Records (common / GEE)	Index	Bias	95% CI of bias	MAE
Dec 2024	4 / 5	NDVI	−0.0005	−0.0018 to +0.0009	0.0059
		EVI	−0.0021	−0.0039 to −0.0003	0.0074
		NDWI	−0.0010	−0.0016 to −0.0004	0.0036
Jan 2025	6 / 8	NDVI	−0.0087	−0.0111 to −0.0063	0.0122
		EVI	−0.0025	−0.0041 to −0.0010	0.0080
		NDWI	+0.0047	+0.0036 to +0.0059	0.0058

Bias = mean of (GEE − common); MAE = mean absolute error. Records are scene–tile records after the cloud filter. Confidence intervals from a block bootstrap (10 × 10 pixel blocks, 2,000 resamples).

3.5 Demonstration area

The public demonstration area reproduced the farm's catalogue reconciliation exactly: 146 GEE records, 136 MPC records, the same ten GEE-only records and the same 22 E2 records. Of the ten E2 pairs with valid pixels, nine had identical SCL and one differed (6 July 2024, T18PXS; validity Jaccard 0.993), a different pair from the farm's. Adding the GEE-only records changed the monthly NDVI medians in all four months tested (Table 4). The January 2025 bias, −0.028, was about three times the farm's, with the same records entering the composite. The size of the effect therefore depends on the area and on how many common scenes are available, and the farm values should not be read as typical.

Table 4. NDVI difference between monthly medians computed with the full GEE inventory and with scenes common to both catalogues over the public demonstration area (same engine, 9,970 pixels).

Month	Records (common / GEE)	Bias	MAE
Sep 2024	1 / 3	+0.0005	0.0130
Dec 2024	4 / 5	+0.0042	0.0074
Jan 2025	6 / 8	−0.0281	0.0284
Feb 2025	5 / 6	−0.0147	0.0150

Bias = mean of (GEE − common); MAE = mean absolute error. Records are scene–tile records after the cloud filter.

4. Discussion

The two platforms were equivalent at the product and processing layers: with the same scenes, they produced the same numbers for the operations tested. The differences we found lay in what each catalogue holds, through two distinct mechanisms: which acquisitions it contains, and which L2A generation of each. The first is catalogue asymmetry. The GEE-only Sentinel-2C records coincide with the satellite's entry into service. A preliminary Sentinel-2C dataset was published from 13 to 19 December 2024, during commissioning (Copernicus Data Space Ecosystem, 2024), and Sentinel-2C replaced Sentinel-2A on 21 January 2025 (Copernicus Data Space Ecosystem, 2025a, 2025b). The 13 December record was acquired on the first day of that publication window, and the 22 January record on the day after the handover. Sentinel-2C products acquired from 13 to 19 December 2024 were first distributed with processing baseline 99.xx and are being republished with the nominal baseline 05.11, after which the 99.xx versions will be removed from the Copernicus catalogue (Copernicus Data Space Ecosystem, 2026). Catalogue inventories for this period are therefore still changing. The GEE-only 13 December records are such products: they carry baseline 99.05, whereas every other GEE-only record carries 05.11. The 11 February 2025 record and the September 2024 Sentinel-2A and 2B records were still absent from MPC as of September 2026 and have no documented explanation, so these interpretations remain inferences.

All extra January scenes were Sentinel-2C. After vicarious adjustment, Sentinel-2C agrees with Sentinel-2A within about 1% in all bands except B12 (Clerc et al., 2026). Part of the January shift could therefore reflect the sensor rather than the number of observations alone; we did not separate the two effects.

The second mechanism is multiple L2A generations of the same acquisition. Reprocessing is a known feature of the Sentinel-2 archive (Enache et al., 2023), but the Collection-1 reprocessing covers acquisitions up to December 2023 and does not explain our June–July 2024 records. Their concentration in seven weeks, with the same baseline and different generation times, suggests that the catalogues ingested different outputs of a reprocessing or re-delivery event that we could not find documented. A different generation rarely changed the usable data, but when it did, the difference lay in the cloud mask, in line with the central role of SCL in defining usable coverage (Sanchez et al., 2024) and with the variability among cloud masks reported in intercomparisons (Skakun et al., 2022).

These results shift the practical question from which platform to use to which scenes a composite contains. Standardising processing across back-ends (Schramm et al., 2021) does not guarantee identical results if the back-ends hold different inventories. A monthly median built from the same code on two platforms can differ by almost 0.01 in mean NDVI over the farm, and by 0.028 over the demonstration area (January 2025), because one catalogue holds an extra acquisition, and that difference is easy to attribute to the platform. In Colombian pastures, Sentinel-2 NDVI is used to estimate forage productivity (Díaz Giraldo et al., 2024); whether a shift of this size matters depends on the slope of such relations and on the change being sought. In our investigation, an initial pairing of scenes by identifier silently dropped the GEE records without an MPC counterpart, and the resulting discrepancy was first read as an implementation effect. The observation-count band stored in the exported composite was the evidence that revealed the extra scenes, whereas image properties set in GEE before export were not present as tags in our GeoTIFF files. These observations support recording provenance inside products and keeping versioned workflows (Groth & Moreau, 2013; Kedron & Frazier, 2022), and citing evolving catalogues through dated queries (Rauber et al., 2016), in line with the FAIR principles (Wilkinson et al., 2016).

The study has limits. It covers one farm and one demonstration area, two tiles and eleven months of catalogue reconciliation, and catalogue contents change over time. The effect on composites was quantified for two months over the farm and four over the demonstration area; months with E2 records were not tested. Each scene–tile record counted as one observation, so acquisitions in the tile overlap weighed twice, and the scene cloud filter used tile-level properties from either catalogue. The magnitude of the effect depends on how many scenes enter a composite and on the processing chain, here a 3 × 3 smoothing and a monthly median. We did not assess annual composites: doing so requires computing the same calendar year from each scene universe and testing equivalence against a pre-specified margin (Schuirmann, 1987; Robinson & Froese, 2004). Finally, products from 2017–2023 may differ between platforms in whether they belong to Collection-1 or to older baselines, which matters for longer series than the one reconciled here.

5. Recommendations

1. Reconcile catalogues before combining them, matching records by acquisition and tile rather than by identifier strings, and decide explicitly on every record present in only one catalogue.
2. Verify product identity: matching dates or datatakes is not sufficient; compare product identifiers.
3. Apply radiometric offsets explicitly and document which convention each source follows.
4. Use a nodata value that cannot be a valid measurement, or a separate mask band.
5. Store provenance inside products: a per-pixel observation count and the list or hash of contributing scenes.
6. Process with one engine and vary only the data source, so that differences can be attributed to data.

7. Record the query date of every reconciliation, because catalogue inventories change.
8. Report the processing baseline of every scene used, because preliminary products, such as early Sentinel-2C data, may be replaced.

6. Conclusions

For the farm studied, GEE and MPC produced Sentinel-2 L2A per-scene indices and monthly medians that agreed within 10^{-6} when given the same scenes: the products and the processing chain tested were equivalent. Differences arose from the scene inventories: some acquisitions, notably from Sentinel-2C, were present only in GEE, and some acquisitions existed in different L2A generations in each catalogue. In the monthly composites tested, these differences shifted mean NDVI by -0.0005 and -0.0087 over the farm and by up to -0.028 over a public demonstration area with the same scene inventory. Combining the platforms is feasible, provided that scene inventories are reconciled and documented. We encourage users to measure the frequency of generation differences and catalogue asymmetry, and their effect on annual composites, in other regions and periods with the data and tools released with this note.

Code and data availability

The reconciliation table with scene identifiers, processing baselines and cloud-cover values; the scene lists, SHA-256 hashes and per-pixel metrics of each composite; the E2 analysis; the evidence tables behind Section 3.2; a public demonstration area of interest; and the three Python tools (MIT licence) with a Spanish-language guide are archived on Zenodo with version 1 of this preprint (https://doi.org/10.5281/zenodo.23241823; text and data under CC BY 4.0, code under the MIT licence). The tools are maintained as an installable Python package with tests and acceptance values for the demonstration area (version 1.1.0: https://doi.org/10.5281/zenodo.23407223; source: https://github.com/hapantevezv-collab/gee-mpc-sentinel2-validation), whose documentation includes a dictionary of every output column. The farm geometry is not shared to protect the landowner's privacy; all scene-level information needed to verify the catalogue findings is included. Sentinel-2 L2A data are openly available from both platforms.

Author contributions

H. A. P. V.: conceptualisation, methodology, software, validation, formal analysis, writing (original draft, review and editing).

Use of generative artificial intelligence

Generative AI assistants were used in preparing this work: Claude (Anthropic, 2026), Opus 5.5 version, and ChatGPT (OpenAI, 2026), GPT-6 and GPT-5.6 Sol models, accessed through a ChatGPT Pro subscription, between September and October 2026. They supported test design, code writing and debugging, literature search, independent review of the manuscript, organisation of results, and drafting and editing of the text. The author defined the research question and scope, ran all code in his own environment, verified the results against the data and reviewed the final content. References were checked against their original sources. The author takes full responsibility for the content.

Competing interests

The author declares no competing interests.

Changes from previous versions

Version 1.1 corrects the December 2024 bias in Table 4 (+0.0042; version 1 reported +0.0043), states both author affiliations, condenses the abstract to 250 words without changing its findings, adds links to the software release and its repository, and removes the acknowledgements. Version 1.2 names the ChatGPT models used and corrects three points found when every reference was checked against its source: the year and title of Rauber et al. (2016), the description of the Sentinel-2C reprocessing (Copernicus Data Space Ecosystem, 2026), which affects products acquired from 13 to 19 December 2024 with baseline 99.xx, and the name of EPSG:9377. Methods, data and conclusions are unchanged.

References

Amani, M., Ghorbanian, A., Ahmadi, S. A., Kakooei, M., Moghimi, A., Mirmazloumi, S. M., Moghaddam, S. H. A., Mahdavi, S., Ghahremanloo, M., Parsian, S., Wu, Q., & Brisco, B. (2020). Google Earth Engine cloud computing platform for remote sensing big data applications: A comprehensive review. *IEEE Journal of Selected Topics in Applied Earth Observations and Remote Sensing, 13*, 5326–5350. https://doi.org/10.1109/JSTARS.2020.3021052

Anthropic. (2026). *Claude* (Opus 5.5 version) [Large language model]. https://claude.ai

Baetens, L., Desjardins, C., & Hagolle, O. (2019). Validation of Copernicus Sentinel-2 cloud masks obtained from MAJA, Sen2Cor, and FMask processors using reference cloud masks generated with a supervised active learning procedure. *Remote Sensing, 11*(4), 433. https://doi.org/10.3390/rs11040433

Bunting, P. [petebunting]. (2022, November 23). *Sentinel-2 BOA_ADD_OFFSET harmonisation* (Issue #134) [Online forum post]. GitHub. https://github.com/microsoft/PlanetaryComputer/issues/134

Clerc, S., Rodat, D., Lafrance, B., Alhammoud, B., Enache, S., Deru, A., Rivoire, L., Adriaensen, S., Hillairet, E., Morrone, R., Iannone, R., & Boccia, V. (2026). Copernicus Sentinel-2C radiometric calibration and validation status. *Remote Sensing, 18*(9), 1387. https://doi.org/10.3390/rs18091387

Copernicus Data Space Ecosystem. (2024, December 13). *Publication of preliminary Sentinel-2C dataset*. https://dataspace.copernicus.eu/news/2024-12-13-publication-preliminary-sentinel-2c-dataset

Copernicus Data Space Ecosystem. (2025a, January 8). *Copernicus Sentinel-2 mission update: Transfer of duty from Sentinel-2A to Sentinel-2C on 21 January 2025*. https://dataspace.copernicus.eu/news/2025-1-8-copernicus-sentinel-2-mission-update-transfer-duty-sentinel-2a-sentinel-2c-21-january

Copernicus Data Space Ecosystem. (2025b, January 17). *Precise timing of transfer of duty from Sentinel-2A to Sentinel-2C on 21 January*. https://dataspace.copernicus.eu/node/2061

Copernicus Data Space Ecosystem. (2026, April 21). *Sentinel-2C reprocessing of tandem data with Sentinel-2A*. https://dataspace.copernicus.eu/node/3214

Díaz Giraldo, R. A., Álvarez de León, M., Pérez López, O., Gutiérrez Parrado, S. L., & Arango Argoti, M. A. (2024). Aplicación de dos modelos basados en teledetección para estimar la producción primaria neta aérea en un sistema pastoril en la Altillanura colombiana. *Tropical Grasslands-Forrajes Tropicales, 12*(1), 24–35. https://doi.org/10.17138/tgft(12)24-35

Drusch, M., Del Bello, U., Carlier, S., Colin, O., Fernandez, V., Gascon, F., Hoersch, B., Isola, C., Laberinti, P., Martimort, P., Meygret, A., Spoto, F., Sy, O., Marchese, F., & Bargellini, P. (2012).

Sentinel-2: ESA's optical high-resolution mission for GMES operational services. *Remote Sensing of Environment, 120*, 25–36. https://doi.org/10.1016/j.rse.2011.11.026

Enache, S., Louis, J., Pflug, B., de los Reyes, R., Lafrance, B., Clerc, S., Barrot, G., Alhammoud, B., Poustomis, F., Iannone, R. Q., Bruniquel, J., Boccia, V., & Gascon, F. (2023). Copernicus Sentinel-2 Collection-1: A consistent dataset of multi-spectral imagery with enhanced quality. In *IGARSS 2023 – 2023 IEEE International Geoscience and Remote Sensing Symposium* (pp. 4302–4305). IEEE. https://doi.org/10.1109/IGARSS52108.2023.10282362

European Space Agency. (n.d.). *S2 processing*. SentiWiki. Retrieved October 8, 2026, from https://sentiwiki.copernicus.eu/web/s2-processing

Flood, N. (2013). Seasonal composite Landsat TM/ETM+ images using the medoid (a multi-dimensional median). *Remote Sensing, 5*(12), 6481–6500. https://doi.org/10.3390/rs5126481

Gomes, V. C. F., Queiroz, G. R., & Ferreira, K. R. (2020). An overview of platforms for big Earth observation data management and analysis. *Remote Sensing, 12*(8), 1253. https://doi.org/10.3390/rs12081253

Google. (n.d.). *Harmonized Sentinel-2 MSI: MultiSpectral Instrument, Level-2A (SR)* [COPERNICUS/S2_SR_HARMONIZED]. Earth Engine Data Catalog. Retrieved September 24, 2026, from https://developers.google.com/earth-engine/datasets/catalog/COPERNICUS_S2_SR_HARMONIZED

Gorelick, N., Hancher, M., Dixon, M., Ilyushchenko, S., Thau, D., & Moore, R. (2017). Google Earth Engine: Planetary-scale geospatial analysis for everyone. *Remote Sensing of Environment, 202*, 18–27. https://doi.org/10.1016/j.rse.2017.06.031

Groth, P., & Moreau, L. (Eds.). (2013). *PROV-Overview: An overview of the PROV family of documents* (W3C Working Group Note). World Wide Web Consortium. https://www.w3.org/TR/prov-overview/

Huete, A., Didan, K., Miura, T., Rodriguez, E. P., Gao, X., & Ferreira, L. G. (2002). Overview of the radiometric and biophysical performance of the MODIS vegetation indices. *Remote Sensing of Environment, 83*(1–2), 195–213. https://doi.org/10.1016/S0034-4257(02)00096-2

IOGP. (n.d.). *EPSG:9377 — MAGNA-SIRGAS 2018 / Origen-Nacional*. EPSG Geodetic Parameter Dataset. Retrieved October 17, 2026, from https://epsg.org/crs/wkt/id/9377

Kedron, P., & Frazier, A. E. (2022). How to improve the reproducibility, replicability, and extensibility of remote sensing research. *Remote Sensing, 14*(21), 5471. https://doi.org/10.3390/rs14215471

Kedron, P., Li, W., Fotheringham, S., & Goodchild, M. (2021). Reproducibility and replicability: Opportunities and challenges for geospatial research. *International Journal of Geographical Information Science, 35*(3), 427–445. https://doi.org/10.1080/13658816.2020.1802032

Main-Knorn, M., Pflug, B., Louis, J., Debaecker, V., Müller-Wilm, U., & Gascon, F. (2017). Sen2Cor for Sentinel-2. In L. Bruzzone, F. Bovolo, & J. A. Benediktsson (Eds.), *Image and signal processing for remote sensing XXIII* (Proceedings of SPIE Vol. 10427, 1042704). SPIE. https://doi.org/10.1117/12.2278218

McFeeters, S. K. (1996). The use of the Normalized Difference Water Index (NDWI) in the delineation of open water features. *International Journal of Remote Sensing, 17*(7), 1425–1432. https://doi.org/10.1080/01431169608948714

Microsoft. (n.d.). *Data catalog*. Microsoft Planetary Computer. Retrieved September 24, 2026, from https://planetarycomputer.microsoft.com/catalog

Nüst, D., & Pebesma, E. (2021). Practical reproducibility in geography and geosciences. *Annals of the American Association of Geographers, 111*(5), 1300–1310. https://doi.org/10.1080/24694452.2020.1806028

Open Geospatial Consortium. (2025). *SpatioTemporal Asset Catalog (STAC) community standard* (Version 1.1, OGC 25-004). http://www.opengis.net/doc/CS/stac/1.1

OpenAI. (2026). *ChatGPT* [Large language model]. https://chatgpt.com

Rauber, A., Asmi, A., Van Uytvanck, D., & Pröll, S. (2016). *Data citation of evolving data: Recommendations of the RDA Working Group on Data Citation (WGDC)*. Research Data Alliance. https://doi.org/10.15497/RDA00016

Robinson, A. P., & Froese, R. E. (2004). Model validation using equivalence tests. *Ecological Modelling, 176*(3–4), 349–358. https://doi.org/10.1016/j.ecolmodel.2004.01.013

Rouse, J. W., Jr., Haas, R. H., Schell, J. A., & Deering, D. W. (1974). Monitoring vegetation systems in the Great Plains with ERTS. In *Third Earth Resources Technology Satellite-1 Symposium: Vol. 1. Technical presentations, section A* (NASA SP-351, pp. 309–317). NASA. https://ntrs.nasa.gov/citations/19740022614

Roy, D. P., Kovalskyy, V., Zhang, H. K., Vermote, E. F., Yan, L., Kumar, S. S., & Egorov, A. (2016). Characterization of Landsat-7 to Landsat-8 reflective wavelength and normalized difference vegetation index continuity. *Remote Sensing of Environment, 185*, 57–70. https://doi.org/10.1016/j.rse.2015.12.024

Sanchez, C., Mena, F., Charfuelan, M., Nuske, M., & Dengel, A. (2024). Assessment of Sentinel-2 spatial and temporal coverage based on the scene classification layer. In *IGARSS 2024 – 2024 IEEE International Geoscience and Remote Sensing Symposium* (pp. 4099–4103). IEEE. https://doi.org/10.1109/IGARSS53475.2024.10642213

Schramm, M., Pebesma, E., Milenković, M., Foresta, L., Dries, J., Jacob, A., Wagner, W., Mohr, M., Neteler, M., Kadunc, M., Miksa, T., Kempeneers, P., Verbesselt, J., Gößwein, B., Navacchi, C., Lippens, S., & Reiche, J. (2021). The openEO API–Harmonising the use of Earth observation cloud services using virtual data cube functionalities. *Remote Sensing, 13*(6), 1125. https://doi.org/10.3390/rs13061125

Schuirmann, D. J. (1987). A comparison of the two one-sided tests procedure and the power approach for assessing the equivalence of average bioavailability. *Journal of Pharmacokinetics and Biopharmaceutics, 15*(6), 657–680. https://doi.org/10.1007/BF01068419

Skakun, S., Wevers, J., Brockmann, C., Doxani, G., Aleksandrov, M., Batič, M., Frantz, D., Gascon, F., Gómez-Chova, L., Hagolle, O., López-Puigdollers, D., Louis, J., Lubej, M., Mateo-García, G., Osman, J., Peressutti, D., Pflug, B., Puc, J., Richter, R., … Žust, L. (2022). Cloud Mask Intercomparison eXercise (CMIX): An evaluation of cloud masking algorithms for Landsat 8 and Sentinel-2. *Remote Sensing of Environment, 274*, 112990. https://doi.org/10.1016/j.rse.2022.112990

Tamiminia, H., Salehi, B., Mahdianpari, M., Quackenbush, L., Adeli, S., & Brisco, B. (2020). Google Earth Engine for geo-big data applications: A meta-analysis and systematic review. *ISPRS Journal of Photogrammetry and Remote Sensing, 164*, 152–170. https://doi.org/10.1016/j.isprsjprs.2020.04.001

Verbesselt, J., Hyndman, R., Newnham, G., & Culvenor, D. (2010). Detecting trend and seasonal changes in satellite image time series. *Remote Sensing of Environment, 114*(1), 106–115. https://doi.org/10.1016/j.rse.2009.08.014

White, J. C., Wulder, M. A., Hobart, G. W., Luther, J. E., Hermosilla, T., Griffiths, P., Coops, N. C., Hall, R. J., Hostert, P., Dyk, A., & Guindon, L. (2014). Pixel-based image compositing for large-area dense time series applications and science. *Canadian Journal of Remote Sensing, 40*(3), 192–212. https://doi.org/10.1080/07038992.2014.945827

Wilkinson, M. D., Dumontier, M., Aalbersberg, Ij. J., Appleton, G., Axton, M., Baak, A., Blomberg, N., Boiten, J.-W., da Silva Santos, L. B., Bourne, P. E., Bouwman, J., Brookes, A. J., Clark, T., Crosas, M., Dillo, I., Dumon, O., Edmunds, S., Evelo, C. T., Finkers, R., … Mons, B. (2016). The FAIR guiding principles for scientific data management and stewardship. *Scientific Data, 3*, 160018. https://doi.org/10.1038/sdata.2016.18

Zhu, Z., & Woodcock, C. E. (2014). Continuous change detection and classification of land cover using all available Landsat data. *Remote Sensing of Environment, 144*, 152–171. https://doi.org/10.1016/j.rse.2014.01.011